

Evolution of two bulk-superconducting phases in $\text{Sr}_{0.5}\text{RE}_{0.5}\text{FBiS}_2$ (RE : La, Ce, Pr, Nd, Sm) by external hydrostatic pressure effect

Aichi Yamashita¹, Rajveer Jha¹, Yosuke Goto¹, Akira Miura², Chikako Moriyoshi³, Yoshihiro Kuroiwa³, Chizuru Kawashima⁴, Kouhei Ishida⁴, Hiroki Takahashi⁴ and Yoshikazu Mizuguchi^{1,*}

¹*Department of Physics, Tokyo Metropolitan University, 1-1 Minami-Osawa, Hachioji, Tokyo, 192-0397, Japan*

²*Faculty of Engineering, Hokkaido University, Kita-13, Nishi-8, Kita-ku, Sapporo, Hokkaido 060-8628, Japan*

³*Graduate School of Advanced Science and Engineering, Hiroshima University, 1-3-1 Kagamiyama, Higashihiroshima, Hiroshima 739-8526, Japan*

⁴*Department of Physics, College of Humanities and Sciences, Nihon University, Setagaya, Tokyo 156-8550, Japan*

Polycrystalline samples of $\text{Sr}_{1-x}\text{RE}_x\text{FBiS}_2$ (RE : La, Ce, Pr, Nd, and Sm) were synthesized via the solid-state reaction and characterized using synchrotron X-ray diffraction. Although all the $\text{Sr}_{0.5}\text{RE}_{0.5}\text{FBiS}_2$ samples exhibited superconductivity at transition temperatures (T_c) within the range of 2.1–2.7 K under ambient pressure, the estimated superconducting volume fraction was small. This indicated the non-bulk nature of superconductivity in these samples under ambient pressure. A dramatic evolution of the bulk superconducting phases was achieved on applying an external hydrostatic pressure. Near pressures below 1 GPa, bulk superconductivity was induced with a T_c of 2.5–2.8 K, which is termed as the low- P phase. Moreover, the high- P phase ($T_c = 10.0$ –10.8 K) featuring bulk characteristics was observed at higher pressures. Pressure- T_c phase diagrams indicated that the critical pressure for the emergence of the high- P phase tends to increase with decreasing ionic radius of the doped RE ions. According to the high-pressure X-ray diffraction measurements of $\text{Sr}_{0.5}\text{La}_{0.5}\text{FBiS}_2$, a structural phase transition from tetragonal to monoclinic also occurred at approximately 1.1 GPa. Thus, this phase transition indicates a pressure-induced superconducting–superconducting transition similar to the transition in $\text{LaO}_{0.5}\text{F}_{0.5}\text{BiS}_2$. Bulk superconducting phases in $\text{Sr}_{0.5}\text{RE}_{0.5}\text{FBiS}_2$ induced by the external hydrostatic pressure effect are expected to be useful for evaluating the mechanisms of superconductivity in BiCh_2 -based superconductors.

Introduction

The discovery of superconductivity in BiS_2 -based compounds such as $\text{Bi}_4\text{O}_4\text{S}_3$ and $\text{REO}_{1-x}\text{F}_x\text{BiS}_2$ has triggered numerous studies focusing on identifying new superconductors featuring a higher transition temperatures (T_c) and elucidating the mechanisms of superconductivity in BiS_2 -based compounds. Due to the similarity between the crystal structures of cuprates and iron-based compounds^{1,2}, BiS_2 -based compounds have been considered as a type of layered superconductors. Thus far, various types of BiS_2 -based compounds have been synthesized by replacing different blocking layers³⁻¹⁴, such as the $\text{Bi}_4\text{O}_4(\text{SO}_4)_{1-x}$ or (REO) (RE : La, Ce, Pr, Nd, and Sm) layers. By manipulating the layered structures, the replacement of (REO) blocking layers with the SrF blocking layers enabled the development of a new class of BiS_2 -based $\text{Sr}_{1-x}\text{RE}_x\text{FBiS}_2$ (RE : La, Ce, Pr, Nd, and Sm) compounds^{12, 15-21}. The parent compound is SrFBiS_2 , which is a semiconductor with a band gap. The substitution of Sr^{2+} with RE^{3+} induces electron carriers in the BiS_2 layer, and filamentary superconductivity appears at approximately 2.8 K in La-, Pr-, and Ce-doped compounds^{12, 17-19}.

Notably, some BiS_2 -based compounds do not exhibit bulk superconductivity even after electron doping. To induce bulk superconductivity in BiS_2 -based compounds, various chemical substitutions have been attempted²²⁻²⁴. Among these, the iso-valent substitutions, such as Nd^{3+} substitutions for La^{3+} or Se^{2-} substitutions for S^{2-} , were found to be effective for inducing bulk superconductivity. Based on systematic structural analyses, we have revealed that the in-plane chemical pressure is one of the essential parameters that facilitate the emergence of bulk superconductivity in BiCh_2 -based (Ch : S, Se) systems^{25,26}.

Regarding the superconducting mechanisms, unconventional pairing mechanisms were suggested based on the recent first principal calculations²⁷⁻²⁹. In addition, angle-resolved photoemission spectroscopy (ARPES) has revealed a strongly anisotropic superconducting gap or the possibility of sign changes in the superconducting gap³⁰. Recently, we have reported the absence of isotope effects on T_c in $\text{LaO}_{0.6}\text{F}_{0.4}\text{BiSSe}$ ³¹, and the two-fold-symmetric in-plane anisotropy of magnetoresistance in the superconducting states in tetragonal $\text{LaO}_{0.5}\text{F}_{0.5}\text{BiSSe}$ with a four-fold-symmetric in-plane structure³². This is likely related to nematic superconductivity states, which have been observed in several unconventional superconductors³³. These findings indicate the emergence of unconventional superconducting states in the $\text{RE(O,F)}\text{BiCh}_2$ system. Therefore, in order to further investigate the superconducting mechanisms of BiCh_2 -based compounds, it is essential to develop a new BiCh_2 -based system.

In this study, we focus on the $\text{Sr}_{0.5}\text{RE}_{0.5}\text{FBiS}_2$ (RE : La, Ce, Pr, Nd, and Sm) system. Based on electrical resistivity measurements conducted under high pressures, a considerable increase in T_c was observed in previous pressure experiments¹⁵⁻¹⁷. The highest T_c in $\text{Sr}_{0.5}\text{RE}_{0.5}\text{FBiS}_2$ is approximately 10 K, and the pressure dependences of T_c exhibits a sharp increase at the critical pressure (~ 1 GPa). It was suggested that the significant increase in T_c under pressure in BiS_2 -based systems was associated with a structural transition from tetragonal to monoclinic, which was revealed via structural analyses of $\text{LaO}_{0.5}\text{F}_{0.5}\text{BiS}_2$ and EuFBiS_2 ^{34,35}. Although there has been no further report on the pressure-induced

superconductivity in $\text{Sr}_{0.5}RE_{0.5}\text{FBiS}_2$, we assumed that a similar structural transition occurs in its case as well. Considering these facts and assumptions regarding the $\text{Sr}_{0.5}RE_{0.5}\text{FBiS}_2$ system, we performed magnetization measurements on the system under high pressures in order to obtain information regarding the superconducting characteristics of both the low- P and high- P phases. Here, we present the evolution of two bulk superconducting phases: the low- P and high- P phases. Furthermore, we characterized the crystal structure of $\text{Sr}_{0.5}\text{La}_{0.5}\text{FBiS}_2$ under high pressures; accordingly, a possible structural transition from tetragonal to monoclinic was observed at approximately 1.1 GPa.

Results

Sample characterization and physical properties at ambient pressure

Fig. 1 depicts the powder synchrotron X-ray diffraction (XRD) patterns for $\text{Sr}_{0.5}\text{La}_{0.5}\text{FBiS}_2$. For $\text{Sr}_{1-x}RE_x\text{FBiS}_2$ ($RE = \text{Ce}, \text{Pr}, \text{Nd}$, and Sm), see supplemental Fig. S1 (a-d). The crystal structure of the obtained samples was well refined using the Rietveld method. They were well refined using a tetragonal structure with the $P4/nmm$ space group. Small impurity peaks due to REF_3 ($RE: \text{La}, \text{Ce}$) and Bi_2S_3 were also detected in the case of the Pr, Nd, Sm-based samples. As shown in Fig. 2, we observed that the lattice constant a decreased with decreasing RE ionic radius; however, the lattice constant c increased under these conditions. The obtained values were in agreement with previous reports^{12, 16}. The chemical composition ratios of the samples were determined using energy dispersive X-ray spectroscopy (EDX). These results showed that the chemical compositions of the obtained samples were in reasonable agreement with the nominal compositions (Table 1). The electrical resistivity of the samples at ambient pressure was measured to be 1.6 K (Fig. 3). The semiconducting behaviour in all the samples was observed; moreover, the $\rho-T$ curve indicated a slight increase in ρ on cooling, which implied that the conduction electrons were weakly localized due to the in-plane local disorder in the BiS_2 layer. A superconducting transition was observed at $T_c = 2.7, 2.7, 2.6, 2.6$, and 2.1 K for $RE = \text{La}, \text{Ce}, \text{Pr}, \text{Nd}$, and Sm , respectively (Fig. 3 inset). In addition, a superconducting transition was also observed in the temperature dependence of magnetization, as plotted in Fig. 4. The T_c estimated based on magnetization was in agreement with that obtained based on the resistivity measurements. This is the first study to report on the observation of superconductivity in $\text{Sr}_{0.5}\text{Nd}_{0.5}\text{FBiS}_2$ and $\text{Sr}_{0.5}\text{Sm}_{0.5}\text{FBiS}_2$ under ambient pressure. However, in these samples, the estimated shielding volume fraction was less than 6%. To obtain bulk superconductivity, which is essentially important for describing intrinsic superconducting properties, we applied external pressure on the samples.

External pressure effect

Fig. 5 (a) shows the temperature dependences of the magnetization of $\text{Sr}_{0.5}\text{La}_{0.5}\text{FBiS}_2$ when increasing the applied pressure to 1.15 GPa. The superconducting transition temperature of approximately 2.7 K (low- P phase) remained almost unchanged up to 0.84 GPa; alternatively, there was an evident increase in the shielding volume fraction. This result indicates that the external pressure effectively enhances the shielding volume fraction, which corresponds to the bulk nature of the

superconducting states in the $\text{Sr}_{0.5}\text{La}_{0.5}\text{FBiS}_2$ samples. A remarkable increase in T_c up to $T_c^{\max} = 10.8$ K (high- P phase) was observed at $P > 0.95$ GPa. This maximum value of T_c is comparable to that obtained for a high- P phase of $\text{LaO}_{0.5}\text{F}_{0.5}\text{BiS}_2^{34,37-39}$ and $\text{Sr}_{0.5}\text{La}_{0.5}\text{FBiS}_2^{15,40}$ through resistivity measurements under high pressure. The enhancement in the shielding volume fraction was also observed in the high- P phase, which was achieved by increasing the applied pressure to the maximum pressure, without a noticeable change in the T_c . Moreover, a similar trend was observed in the low- P region. The drastic increase in T_c is likely related to the structural transition from a tetragonal to a monoclinic phase, which was suggested for the related superconductor $\text{LaO}_{0.5}\text{F}_{0.5}\text{BiS}_2$ based on the XRD under high pressure³⁴. The pressure dependence of T_c is summarized in Fig. 5 (f); the light blue, blue, and pink regions indicate the filamentary superconductivity, bulk superconductivity in the low- P phase, and bulk superconductivity in the high- P phase, respectively. The low- P phase shifts to the high- P phase when a pressure slightly exceeding the critical pressure (P_c) for the high- P phase is applied. In regard to this, a phase diagram was created using the shielding volume fraction of 20% or more as a bulk state in order to discuss the phase transition. In the pressure range of 0–0.84 GPa, $T_c(P)$ remains almost constant (~ 2.7 K). The bulk superconductivity of the sample was induced by the pressure for the low- P phase region; eventually, the high- P phase region emerged at approximately $P = 0.95$ GPa with the bulk superconducting states. The $T_c(P)$ for the high- P phase region is almost constant (10.8 K). The temperature dependence of magnetization under pressure and the pressure dependence of T_c phases for all the samples are summarized in Fig. 5 (a-e) and (f-j), respectively. The high- P phase of $\text{Sr}_{0.5}\text{Sm}_{0.5}\text{FBiS}_2$ was not observed up to 1.28 GPa, which is nearly the upper limit of the pressure measurement apparatus used in this experiment. This is the first report offering evidence of the bulk nature of two different (low- and high- P) phases of the $\text{Sr}_{1-x}\text{RE}_x\text{FBiS}_2$ (RE : La, Ce, Pr, Nd, and Sm) superconductors when subjected to pressure.

Discussion

In this section, we discuss the relationship between external pressure effects, chemical pressure effects, and evolution of superconductivity in $\text{Sr}_{0.5}\text{RE}_{0.5}\text{FBiS}_2$. On comparing the evolutions of superconductivity for $\text{RE} = \text{Ce-Sm}$ and that for $\text{RE} = \text{La}$, a slight decrease in T_c for the low- P phase was observed with increasing pressure for the $\text{RE} = \text{Ce, Pr, Nd}$ and, Sm samples. This deviation in the behaviour might be explained by the effect of coexistence of both the external as well as chemical pressures²⁵. Moreover, we observed that the T_c of the high- P phase varied slightly with the RE ionic radius. On the contrary, the P_c for the high- P phase increased with decreasing RE ionic radius. Specifically, assuming a coordination number of 8, P_c was roughly estimated as 0.95, 1.11, 1.17, and 1.33 GPa for La^{3+} (with an ionic radius of 1.16 Å), Ce^{3+} (with an ionic radius of 1.14 Å), Pr^{3+} (with an ionic radius of 1.13 Å), and Nd^{3+} (with an ionic radius of 1.11 Å), respectively. The tendency of the increase in P_c and the decrease in T_c with a decrease in RE ionic radius was also observed for $\text{REO}_{0.5}\text{F}_{0.5}\text{BiS}_2$ compounds^{38,39,40}; specifically, the T_c varied from approximately 10 K to 6 K, and a significantly higher P_c was required with decreasing RE ionic radius. These observations highlight the

relationship between the structural transition to monoclinic and the packing density in the BiS₂ conducting layers³⁴. It is possible that the larger space along the BiS conduction plane with a larger *RE* ionic radius possibly transmits the pressure, thereby inducing structural transition. As shown in Fig. 6, T_c^{mag} of all samples for the low- and high-*P* phases were plotted with respect to the lattice constant *a*. T_c of the high-*P* phase was defined as the highest T_c for the range of applied pressures, whereas T_c of the low-*P* phase was defined as the value of T_c when the applied pressure is lower than the pressure for the emergency of the high-*P* phase. A slightly increasing trend in T_c was observed for both low- and high-*P* phases with increasing lattice constant *a* estimated under an ambient pressure.

Fig. 7 (a) presents the X-ray diffraction patterns of Sr_{0.5}La_{0.5}FBiS₂ at room temperature under various applied pressures of up to 3.4 GPa. Shifts of the (001) and (004) peaks to higher angles clearly indicate the shrinkage of the lattice along the *c*-axis due to the pressure. In contrast, a relatively smaller shift of the (110) peak was detected, which indicates that the in-plane size remains almost unchanged. Strong peak broadening was observed for the (200) peak above 1.1 GPa, indicating peak splitting due to the lowering of in-plane structural symmetry. Similar peak splitting on the (200) peak was observed for isostructural LaO_{0.5}F_{0.5}BiS₂ and EuFBiS₂ samples under high pressure^{34,35,41}, and a resultant structural transition from a tetragonal to monoclinic phase was detected. We noticed that the (200) peak asymmetrically split into two or more peaks, as depicted in Fig. 7 (b). This may be due to the inhomogeneity of applied pressure and the flexible nature of the in-plane structure of BiS₂-based compounds. The critical pressure of 1.1 GPa estimated from the XRD corresponds satisfactorily with the P_c estimated from the magnetization measurements.

Conclusion

Herein, we report on the results of the crystal structure, resistivity, and magnetic susceptibility under pressure for (Sr,*RE*)FBiS₂ (*RE*: La, Ce, Pr, Nd, and Sm). The effects of external pressure on magnetization resulted in abrupt increments in T_c up to 10–10.8 K, for samples with *RE* = La, Ce, Pr, and Nd. Based on analyses of the shielding volume fraction estimated via magnetic susceptibility measurements, we found that two bulk superconducting phases (low-*P* and high-*P* phases) existed for (Sr,*RE*)FBiS₂. The common features were that the bulk low-*P* phase was induced by external pressure, whereas the bulk high-*P* phase was induced at pressures exceeding a critical pressure. Moreover, at the critical pressure, T_c sharply increased to the high-*P* phase as our experiment shifted to higher pressures with decreasing *RE* ionic radius; this implied that both the external as well as chemical pressures were affecting T_c . In addition, we investigated the variations in the crystal structure under pressure. By analysing the splitting of the (200) peak, we concluded that the high-*P* phase was a monoclinic structure. Various bulk superconducting phases with different space group induced via external pressure effects in (Sr,*RE*)FBiS₂ need to be further investigated in order to elucidate the mechanisms of superconductivity in BiCh₂-based systems.

Methods

Polycrystalline Sr_{0.5}*RE*_{0.5}FBiS (*RE*: La, Ce, Pr, Nd, and Sm) samples were synthesized by solid state

reaction method in an evacuated quartz tube. Powders of RE_2S_3 (RE : La (99.9%), Ce (99.9%), Pr (99%), Nd (99%), and Sm (99.9%)), SrF_2 (99%), Bi (99.999%), and S (99.9999%) were weighed for $Sr_{0.5}RE_{0.5}FBiS_2$. The mixed powder was subsequently pelletized, sintered in an evacuated quartz tube at 700°C for 20 hours, followed by furnace cooling to room temperature. The obtained compounds were thoroughly mixed and ground, then sintered in the same conditions at the first sintering.

The phase purity and the crystal structure of the $Sr_{1-x}RE_xFBiS_2$ (RE : La, Ce, Pr, Nd, and Sm) samples were examined by powder synchrotron XRD with an energy of 25 keV ($\lambda = 0.49657 \text{ \AA}$) at the beamline BL02B2 of SPring-8 under a proposal No. 2019A1101. The synchrotron XRD experiments were performed at room temperature with a sample rotator system, and the diffraction data were collected using a high-resolution one-dimensional semiconductor detector MYTHEN [Multiple mythen system] with a step of $2\theta = 0.006^\circ$. To investigate the crystal structure of $Sr_{0.5}La_{0.5}FBiS_2$, XRD experiments under high pressure up to 3.4 GPa were performed at room temperature using a Mo-K α radiation on a Rigaku (MicroMax-007HF) rotating anode generator equipped with a 100 μm collimator. Daphne 7474 was used as a pressure medium.

The crystal structure parameters were refined using the Rietveld method with a RIETAN-FP software³⁶. The actual compositions of the obtained samples were analyzed using an energy dispersive X-ray spectroscopy (EDX) on TM-3030 (Hitachi).

The temperature dependence of magnetic susceptibility at ambient pressure and under high pressures were measured using a superconducting quantum interference devise (SQUID) with MPMS-3 (Quantum Design). Hydrostatic pressures were generated by the MPMS high pressure Capsule Cell. The sample was immersed in a pressure transmitting medium (Daphene 7373) covered with a Teflon cell. The pressure at low temperature was calibrated from the superconducting transition temperature of Pb manometer. The electrical resistivity was measured on a GM refrigerator system (Made by Axis) using a conventional four-probe method. For the resistivity measurements, gold wires were connected to the samples with a silver paste.

References

1. Bednorz, J. G. & Müller, K. A. Possible high T_c superconductivity in the Ba-La-Cu-O system. *Z. Phys. B* **64**, 189–193 (1986).
2. Kamihara, Y., Watanabe, T., Hirano, M. & Hosono, H. Iron-based layered superconductor $La[O_{1-x}F_x]FeAs$ ($x = 0.05$ –0.12) with $T_c = 26$ K. *J. Am. Chem. Soc.* **130**, 3296–3297 (2008).
3. Mizuguchi, Y. et al. BiS_2 -based layered superconductor $Bi_4O_4S_3$. *Phys. Rev. B* **86**, 220510(R) (2012).
4. Mizuguchi, Y. et al. Superconductivity in novel BiS_2 -based layered superconductor $LaO_{1-x}F_xBiS_2$. *J. Phys. Soc. Jpn.* **81**, 114725 (2012).
5. Singh, S. K. et al. Bulk superconductivity in bismuth oxysulfide $Bi_4O_4S_3$. *J. Am. Chem. Soc.* **134**, 16504–16507 (2012).
6. Demura, S. et al. BiS_2 -based superconductivity in F-substituted $NdOBiS_2$. *J. Phys. Soc. Jpn.* **82**,

1–3 (2013).

7. Jha, R., Kumar, A., Singh, S. K. & Awana, V. P. S. Synthesis and superconductivity of new BiS₂ based superconductor PrO_{0.5}F_{0.5}BiS₂. *J. Supercond. Nov. Magn.* **26**, 499–502 (2013).
8. Jha, R., Kumar, A., Singh, S. K. & Awana, V. P. S. Superconductivity at 5 K in NdO_{0.5}F_{0.5}BiS₂. *J. Appl. Phys.* **113**, 056102 (2013).
9. Xing, J., Li, S. Ding, X., Yang, H. & Wen, H. H. Superconductivity appears in the vicinity of an insulating-like behavior in CeO_{1-x}F_xBiS₂. *Phys. Rev. B* **86**, 214518 (2012).
10. Yazici, D. et al. Superconductivity of F-substituted *Ln*OBiS₂ (*Ln* = La, Ce, Pr, Nd, Yb) compounds. *Philos. Mag.* **93**, 673 (2012).
11. Yazici, D. et al. Superconductivity induced by electron doping in La_{1-x}M_xOBiS₂ (M = Ti, Zr, Hf, Th). *Phys. Rev. B* **87**, 174512 (2013).
12. Lin, X. et al. Superconductivity induced by La doping in Sr_{1-x}La_xFBiS₂. *Phys. Rev. B* **87**, 020504 (2013).
13. Mizuguchi, Y. Review of superconductivity in BiS₂-based layered materials. *J. Phys. Chem. Solids* **84**, 34–48 (2015).
14. Mizuguchi, Y., Material Development and physical properties of BiS₂-based layered Compounds. *J. Phys. Soc. Jpn.* **88**, 041001 (2019).
15. Jha, R., Tiwari, B. & Awana, V. P. S. Impact of hydrostatic pressure on superconductivity of Sr_{0.5}La_{0.5}FBiS₂. *J. Phys. Soc. Jpn.* **83**, 063707 (2014).
16. Jha, R., Tiwari, B. & Awana, V. P. S. Appearance of bulk superconductivity under hydrostatic pressure in Sr_{0.5}RE_{0.5}FBiS₂ (RE = Ce, Nd, Pr, and Sm) compounds. *J. Appl. Phys.* **117**, 013901 (2015).
17. Jha, R. & Awana V.P.S. Effect of hydrostatic pressure on BiS₂-based layered superconductors: a review. *Nov. Supercond. Mater.* **2**, 16-31 (2016).
18. You, W. et al. Superconductivity, electronic phase diagram, and pressure effect in Sr_{1-x}Pr_xFBiS₂. *Sci. China-Phys. Mech. Astron.* **62**, 957411 (2019).
19. Li, L. et al. Coexistence of superconductivity and ferromagnetism in Sr_{0.5}Ce_{0.5}FBiS₂. *Phys. Rev. B* **91**, 014508 (2015).
20. Hideaki, S. et al. Insulator-to-superconductor transition upon electron doping in a BiS₂-based superconductor Sr_{1-x}La_xFBiS₂. *J. Phys. Soc. Jpn.* **83**, 014709 (2014).
21. Lei, H., Wang, K., Abeykoon, M., Bozin, E. S. & Petrovic C. New layered fluorosulfide SrFBiS₂. *Inorg. Chem.* **52**, 10685-10689 (2013).
22. Goto, Y., Sogabe, R. & Mizuguchi, Y. Bulk superconductivity induced by Se substitution in BiCh₂-based layered compounds Eu_{0.5}Ce_{0.5}FBiS_{2-x}Se_x. *J. Phys. Soc. Jpn.* **86**, 104712 (2017).
23. Jinno, Y. et al. Bulk superconductivity induced by in-plane chemical pressure effect in Eu_{0.5}La_{0.5}FBiS_{2-x}Se_x. *J. Phys. Soc. Jpn.* **85**, 124708 (2016).
24. Li, L. et al. Superconductivity and abnormal pressure effect in Sr_{0.5}La_{0.5}FBiSe₂ superconductor. *Supercond. Sci. Technol.* **29**, 04LT03 (2016).

25. Mizuguchi, Y. et al., In-plane chemical pressure essential for superconductivity in BiCh_2 -based (Ch : S, Se) layered structure. *Sci. Rep.* **5**, 14968 (2015).
26. Mizuguchi Y. Material development and physical properties of BiS_2 -based layered compounds. *J. Phys. Soc. Jpn.* **88**, 041001 (2019).
27. Morice, C., Akashi, R., Koretsune, T., Saxena, S. S. & Arita, R. Weak phonon-mediated pairing in BiS_2 superconductor from first principles. *Phys. Rev. B* **95**, 180505 (R) (2017).
28. Suzuki, K., Usui, H., Kuroki, K. & Ikeda H. Charge and quadrupole fluctuations and gap anisotropy in BiS_2 -based superconductors. *Phys. Rev. B* **96**, 024513 (2017).
29. Suzuki, K. et al. Electronic structure and superconducting gap structure in BiS_2 -based layered superconductors. *J. Phys. Soc. Jpn.* **88**, 041008 (2019).
30. Ota, Y. et al. Unconventional superconductivity in the BiS_2 -based layered superconductor $\text{NdO}_{0.71}\text{F}_{0.29}\text{BiS}_2$. *Phys. Rev. Lett.* **118**, 167002 (2017).
31. Hoshi, K., Goto, Y. & Mizuguchi, Y. Selenium isotope effect in layered bismuth chalcogenide superconductor $\text{LaO}_{0.6}\text{F}_{0.4}\text{Bi}(\text{S},\text{Se})_2$. *Phys. Rev. B* **97**, 094509 (2018).
32. Hoshi, K., Kimata, M., Goto, Y., Matsuda, T. D. & Mizuguchi, Y. Two-fold-symmetric magnetoresistance in single crystals of tetragonal BiCh_2 -based superconductor $\text{LaO}_{0.5}\text{F}_{0.5}\text{BiSSe}$. *J. Phys. Soc. Jpn.* **88**, 033704 (2019).
33. Shingo, Y. Nematic superconductivity in doped Bi_2Se_3 topological superconductors. *Condens. Matter* **4**, 2 (2019).
34. Tomita, T. et al. Pressure-induced enhancement of superconductivity and structural transition in BiS_2 -layered $\text{LaO}_{1-x}\text{F}_x\text{BiS}_2$. *J. Phys. Soc. Jpn.* **83**, 063704 (2014).
35. Guo, C.Y. et al. Evidence for two distinct superconducting phases in EuBiS_2F under pressure. *Phys. Rev. B* **91**, 214512 (2015).
36. Izumi, F. & Momma, K. Three-dimensional visualization in powder diffraction. *Solid State Phenom.* **130**, 15-20 (2007).
37. Hisashi, K. et al. Pressure study of BiS_2 -based superconductors $\text{Bi}_4\text{O}_4\text{S}_3$ and $\text{La}(\text{O},\text{F})\text{BiS}_2$. *J. Phys. Soc. Jpn.* **81**, 103702 (2012).
38. Wolowiec, C.T., Yazici, D., White, B. D., Huang, K. & Maple, M. B. Pressure-induced enhancement of superconductivity and suppression of semiconducting behavior in $\text{LnO}_{0.5}\text{F}_{0.5}\text{BiS}_2$ ($\text{Ln} = \text{La, Ce}$) compounds. *Phys. Rev. B* **88**, 064503 (2013).
39. Jha, R., Kishan H. & Awana V.P.S. Effect of hydrostatic pressures on the superconductivity of new BiS_2 based $\text{REO}_{0.5}\text{F}_{0.5}\text{BiS}_2$ ($\text{RE}=\text{La, Pr and Nd}$) superconductors. *Journal of Physics and Chemistry of Solid* **84**, 17-23 (2015).
40. Wolowiec, C. T. et al. Enhancement of superconductivity near the pressure-induced semiconductor–metal transition in the BiS_2 -based superconductors $\text{LnO}_{0.5}\text{F}_{0.5}\text{BiS}_2$ ($\text{Ln} = \text{La, Ce, Pr, Nd}$). *J. Phys.: Condens. Matter* **25**, 422201 (2013).
41. Mizuguchi, Y. et al. Stabilization of high- T_c phase of BiS_2 -based superconductor $\text{LaO}_{0.5}\text{F}_{0.5}\text{BiS}_2$ using high-pressure synthesis. *J. Phys. Soc. Jpn.* **83**, 053704 (2014).

Acknowledgments

The authors thank O. Miura for experimental supports. This work was partly supported by JSPS KAKENHI (Grant No. 18KK0076, 15H05886, and 19K15291) and Advanced Research Program under the Human Resources Funds of Tokyo (Grant Number: H31-1) and Nihon University President Grant Initiative.

Author Contributions

A.Y. prepared all samples and did compositional analysis, resistivity, magnetization measurements. A.Y. measured magnetization under high pressure with the help of R.J. A.M., C.M. and Y.K. conducted powder synchrotron XRD measurements. C.K., K.I. and H.T. conducted the high-pressure XRD measurements. A.Y. wrote the manuscript and prepared all figures. Y.G. and Y.M. provided valuable suggestion for data analysis and corrected the manuscript. All authors contributed to discussion and reviewed the manuscript.

Additional Information

Competing Interests: The authors declare no competing interests.

Publishing's note Springer Nature remains neutral with regard to jurisdictional claims in published maps and institutional affiliations.

Figures

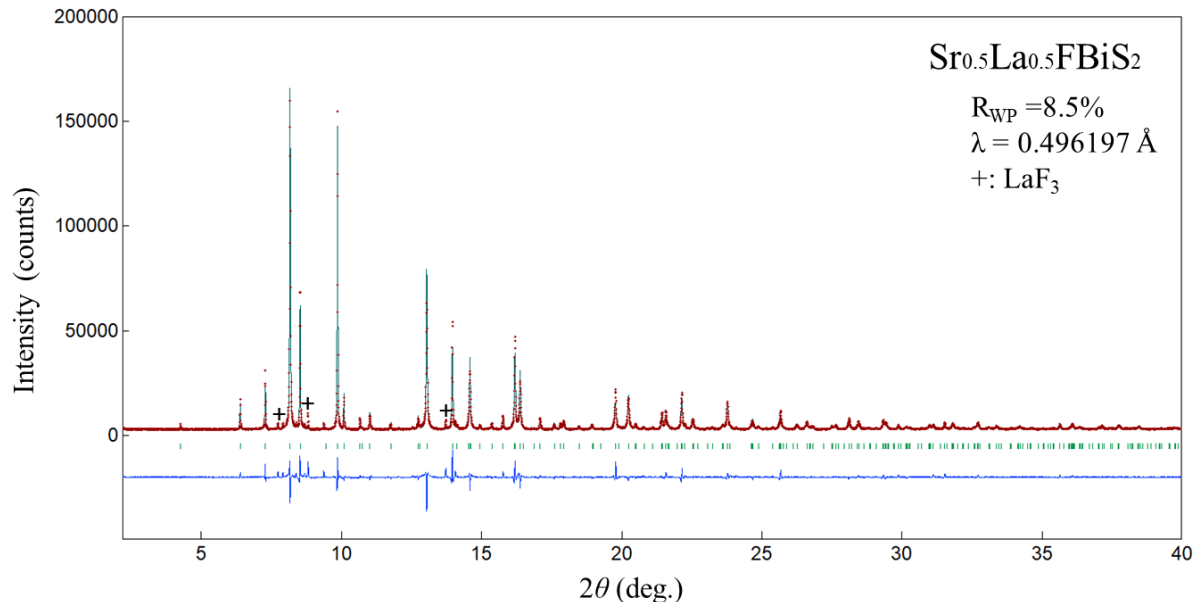


Fig.1 SXRD patterns for $\text{Sr}_{0.5}\text{La}_{0.5}\text{FBiS}_2$. Symbol of + indicates the impurity of LaF_3 .

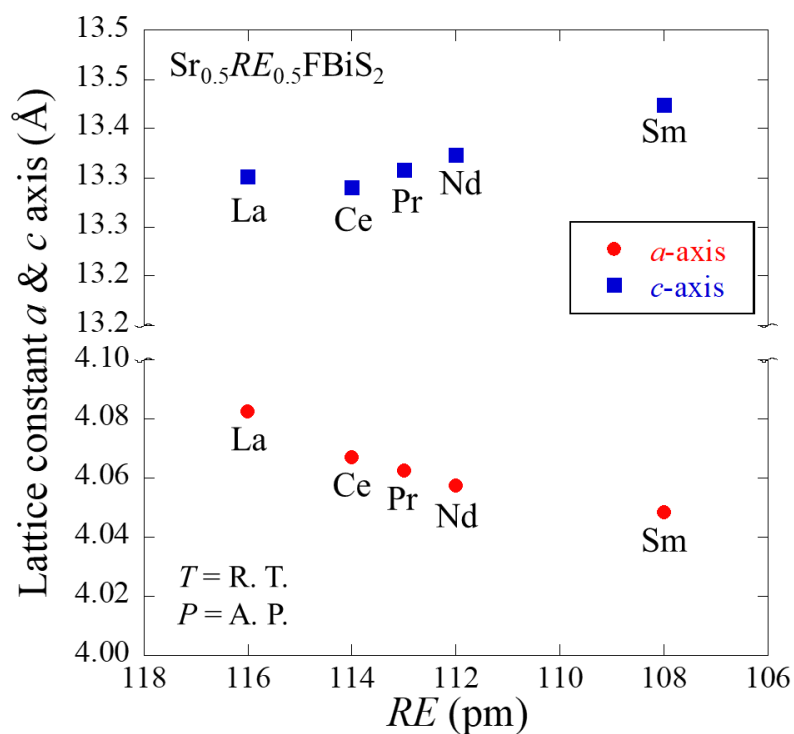


Fig.2 Dependences of the lattice constants a and c as a function of the RE^{3+} (RE : La, Ce, Pr, Nd, and Sm) ionic radius.

Nominal composition	Actual composition
$\text{Sr}_{0.50}\text{La}_{0.50}\text{FBiS}_2$	$\text{Sr}_{0.52}\text{La}_{0.48}\text{FBi}_{1.00}\text{S}_{2.00}$
$\text{Sr}_{0.50}\text{Ce}_{0.50}\text{FBiS}_2$	$\text{Sr}_{0.54}\text{Ce}_{0.48}\text{FBi}_{0.98}\text{S}_{2.00}$
$\text{Sr}_{0.50}\text{Pr}_{0.50}\text{FBiS}_2$	$\text{Sr}_{0.56}\text{Pr}_{0.41}\text{FBi}_{0.99}\text{S}_{2.04}$
$\text{Sr}_{0.50}\text{Nd}_{0.50}\text{FBiS}_2$	$\text{Sr}_{0.60}\text{Nd}_{0.39}\text{FBi}_{0.98}\text{S}_{2.03}$
$\text{Sr}_{0.50}\text{Sm}_{0.50}\text{FBiS}_2$	$\text{Sr}_{0.64}\text{Sm}_{0.39}\text{FBi}_{0.97}\text{S}_{2.01}$

Table 1 Actual composition (mol%) from the EDX analysis against the nominal composition (mol%). Fluorine amount is regarded as 1.

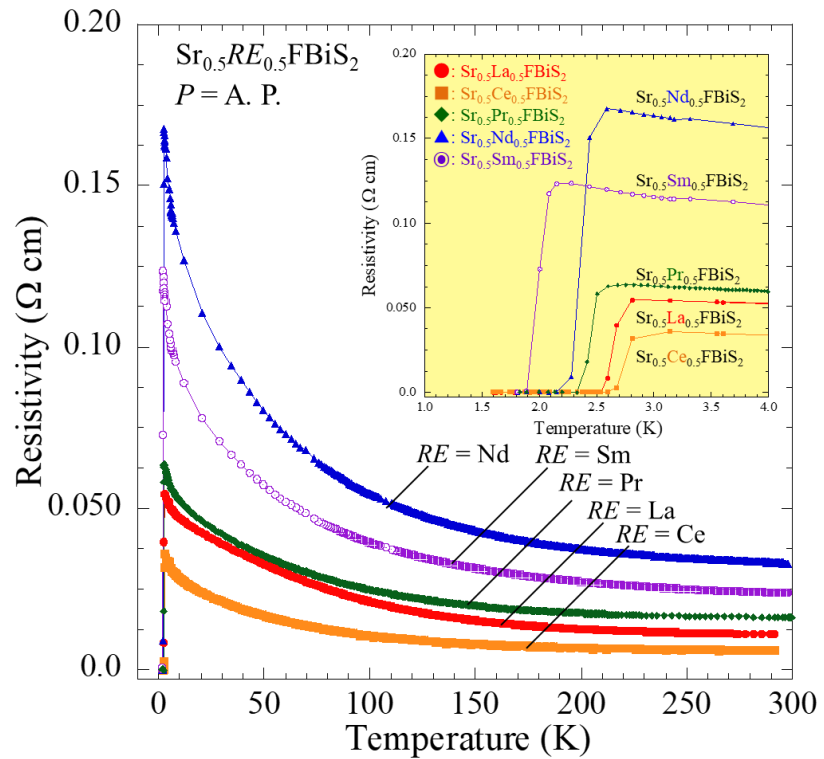


Fig. 3 Temperature dependence of resistivity for $\text{Sr}_{1-x}\text{RE}_x\text{FBiS}_2$ (RE : La, Ce, Pr, Nd, and Sm) at ambient pressure.

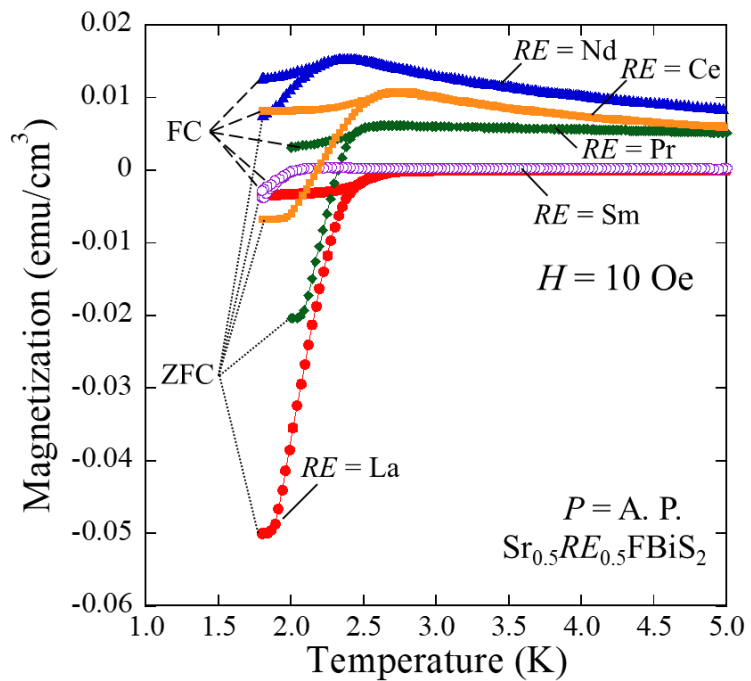


Fig.4 Temperature dependence of magnetization for $\text{Sr}_{1-x}\text{RE}_x\text{FBiS}_2$ (RE : La, Ce, Pr, Nd, and Sm) at ambient pressure. Dashed and dotted lines indicate a field cooling (FC) and zero field cooling (ZFC), respectively.

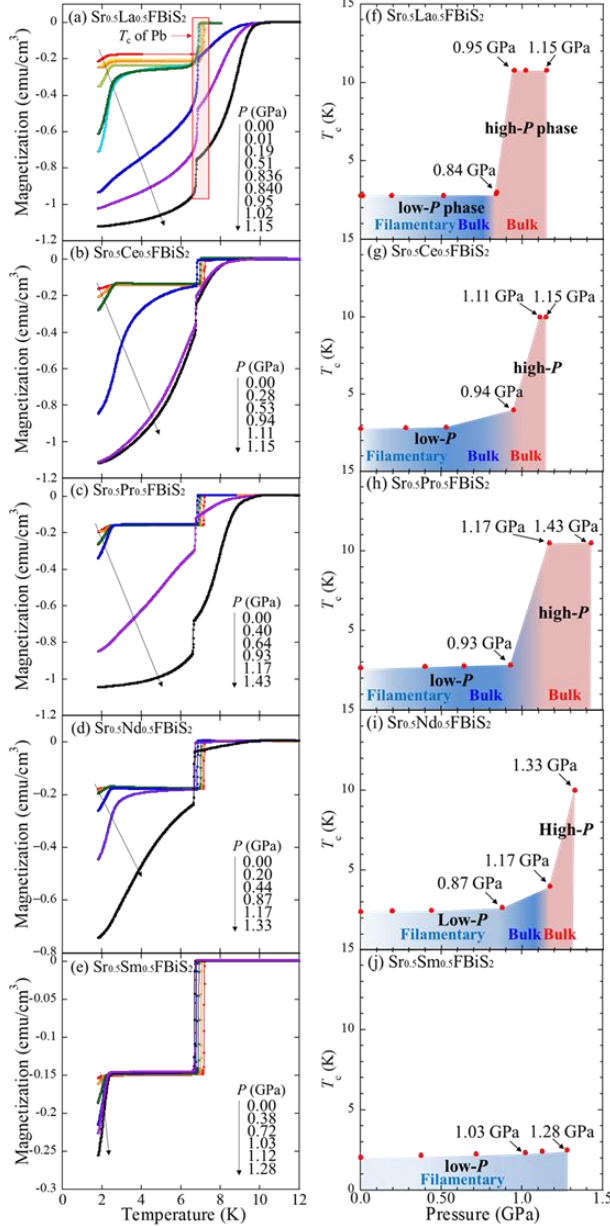


Fig.5 (a-e) Temperature dependence of magnetization under various pressure ($P_{\text{La}} = 0, 0.01, 0.19, 0.51, 0.836, 0.840, 0.95, 1.02, 1.15 \text{ GPa}$; $P_{\text{Ce}} = 0, 0.28, 0.53, 0.94, 1.11, 1.15 \text{ GPa}$; $P_{\text{Pr}} = 0.0, 0.40, 0.64, 0.93, 1.17, 1.43 \text{ GPa}$; $P_{\text{Nd}} = 0.0, 0.20, 0.44, 0.87, 1.17, 1.33 \text{ GPa}$; $P_{\text{Sm}} = 0.0, 0.375, 0.716, 1.03, 1.12, 1.28 \text{ GPa}$) for $\text{Sr}_{0.5}\text{RE}_{0.5}\text{FBiS}_2$ (RE : La, Ce, Pr, Nd, and Sm), (f-j) Pressure dependence of T_c for $\text{Sr}_{0.5}\text{RE}_{0.5}\text{FBiS}_2$ (RE : La, Ce, Pr, Nd, and Sm). Magnetic fields of 10 Oe are applied for all samples. Transition around 7 K indicates the superconducting transition of Pb manometer.

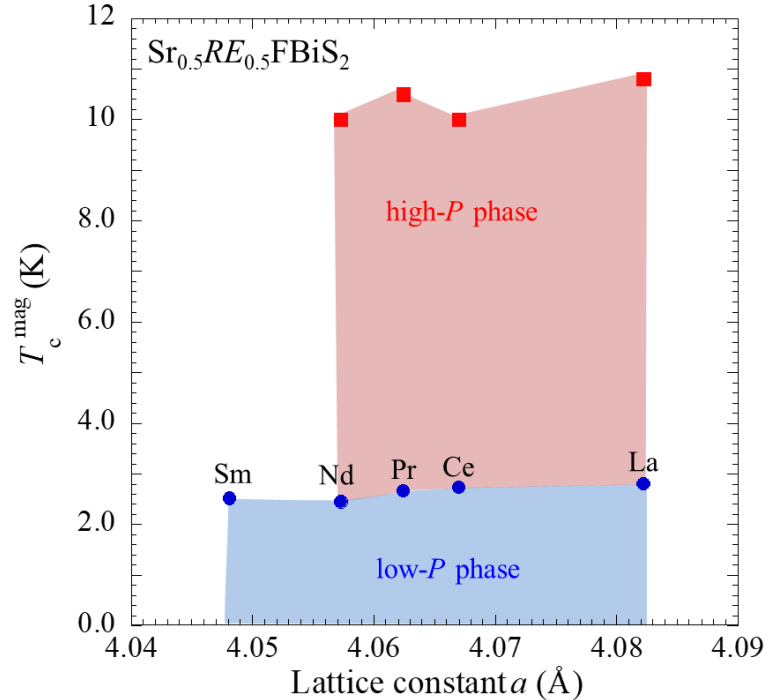


Fig.6 T_c for both low- and high- P phases against the lattice constant a at an ambient pressure.

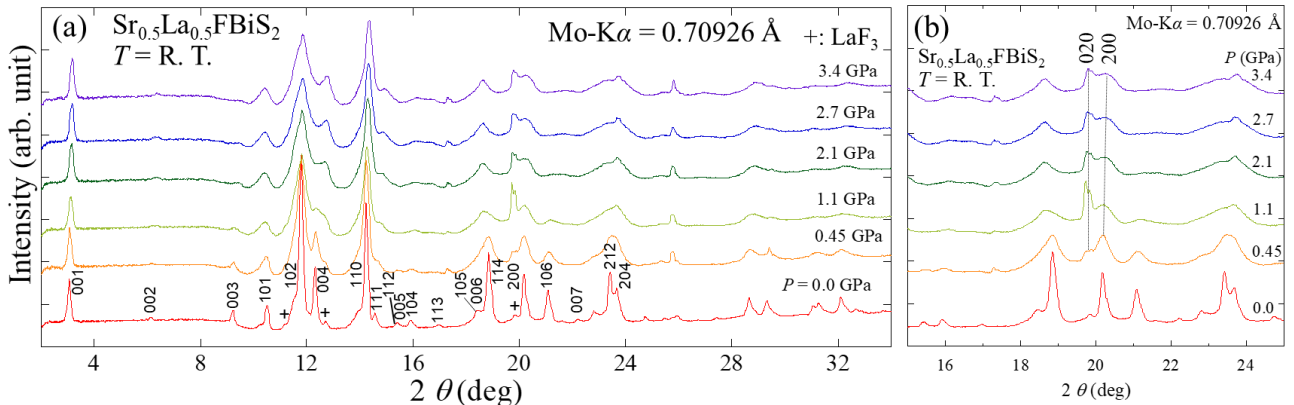


Fig. 7(a) XRD patterns ($\text{Mo K}\alpha$) of $\text{Sr}_{0.5}\text{La}_{0.5}\text{FBiS}_2$ under various pressure at room temperature. (b) Zoomed XRD patterns near the 020 and 200 peaks.